A Magnetic Multi-Enzyme@Metal-Organic Material (MOM) for Sustainable Biodegradation of Insoluble Biomass

Mary Lenertz,[1] Qiaobin Li, [1] Zoe Armstrong,[1] Allison Scheiwiller,[1] Gigi Ni,[2] Jien Wang,[3] Li Feng,[1] Austin MacRae,[1,*] and Zhongyu Yang[1,*]

1. Department of Chemistry and Biochemistry, North Dakota State University, Fargo, ND, USA 58102

2. Department of Chemistry and Chemical Biology, Harvard University, Boston, MA, USA 02138

3. California State University, San Marcos, San Marcos, CA, USA 92096

Corresponding to: zhongyu.yang@ndsu.edu

austin.macrae@ndsu.edu

Abstract

Biodegradation of insoluble biomass such as cellulose via carbohydrase enzymes is an effective approach to break down plant cell walls and extract valuable materials therein. Yet the high cost and poor reusability of enzymes are practical concerns. We recently proved that immobilizing multiple digestive enzymes on metal-organic materials (MOMs) allows enzymes to be reused via gravimetric separation, improving the cost efficiency of cereal biomass degradation [*ACS Appl. Mater. Interfaces 2021, 13, 36, 43085–43093*]. However, this strategy cannot be adapted for enzymes whose substrates/products are insoluble (e.g., cellulose crystals). Recently, we described an alternative approach based on magnetic Metal-Organic Frameworks (MOFs) work using model enzymes/substrates [*ACS Appl. Mater. Interfaces 2020, 12, 37, 41794–41801*]. Here, we aim at proving the effectiveness of combining these two strategies in cellulose degradation. We immobilized multiple carbohydrase enzymes that cooperate in cellulose degradation via co-crystallization with Ca^{2+}, a carboxylate ligand (BDC) in the absence and presence of magnetic nanoparticles (MNPs). We then compared the separation efficiency and enzyme reusability of the resultant multi-enzyme@Ca-BDC and multi-enzyme@MNP-Ca-BDC composites via gravimetric and magnetic separation, respectively, and found that, although both composites were effective in cellulose degradation in the first round, the multi-enzyme@MNP-Ca-BDC composites displayed significantly enhanced reusability. This work provides the first experimental demonstration of using magnetic solid supports to immobilize multiple carbohydrase enzymes simultaneously and degrade cellulose and promotes green/sustainable chemistry in three folds: 1) reusing the enzymes saves energy/sources to prepare them, 2) the synthetic conditions are “green” without generating unwanted wastes, and 3) using our composites to degrade cellulose is the first step of extracting

valuable materials from sustainable biomasses such as plants whose growth does not rely on non-regeneratable resources.

Keywords: metal-organic materials (MOMs); magnetic MOMs; magnetic MOFs; cellulose biodegradation; cellulase immobilization; hemicellulase immobilization;

Introduction

Plants are ample and sustainable natural sources of (bio)fuels, (bio)materials, and nutrients whose growth only relies on sunlight, soil, and rain/water.[1-5] However, most of the valuable components in plants such as sugar/polysaccharides, food proteins, chemicals, and fuels are buried under the intensely packed, "protection" layers of plant cell walls,[6-7] the dominant compositions of which are cellulose, hemicellulose, and other oligosaccharides.[8-10] Thus, to extract the valuable natural substances from plants, a prerequisite is to breakdown the cellulose network. While chemical breaking-down may be the first option in mind, it is suffered from the difficulty in controlling the reaction extent and minimizing damage to the valuable components or unwanted by-products;[7, 11-16] biodegradation via microorganisms (especially their carbohydrase enzymes that function cooperatively to degrade polysaccharides) is more selective and biocompatible.[8-10, 17] However, this approach requires special expertise on microbiology and can be challenged by the difficulty in controlling microorganisms' performance. Extracting and simultaneously applying all needed enzymes can simplify the procedure with more controlled performance, yet the high cost to prepare and maintain the enzymes become a practical barrier.[10, 18-37] Immobilizing enzymes on solid supports can improve the cost-efficiency, yet depends heavily on the immobilizing methods, which may cause leaching (if physically attached) or enzyme alteration (if chemically linked).[30-40] Porous nanomaterials may overcome both but not applicable to large substrates such as cellulose which cannot diffuse into the pores.[32, 38-40] All solid supports are challenged when enzymes' substrates/products possess low solubilities when attempting to reuse the enzymes@solid supports.

Metal-Organic Frameworks/Materials (MOFs/MOMs) are unique platforms to immobilize enzymes in their pores.[41-52] For enzymes and substrates larger than MOF/MOM pores, co-crystallization of enzymes and metal ions/ligands can be applied[53-55] wherein enzymes are partially

"rooted" under the MOF/MOM surfaces and partially exposed to contact the reaction medium and thus, large substrates.[54, 56-58] MOFs/MOMs offer high reusability of the implanted enzymes and partial protection (the buried section of the enzymes) so that harsher experimental conditions can be applied to speed up reactions.[53-55] Some MOMs can be synthesized in the aqueous phase with high stability under both acidic and basic conditions,[53] in comparison to ZIF-859 and UiO-66,[60] and are thus,[61-66] become optimal to immobilize multiple enzymes on the same surface.[53, 55, 58] We have recently demonstrated this strategy on a few enzymes and a digestive enzyme-cluster whose enzymes cooperate in a cascade manner to degrade cereal biomass.[53, 56, 58, 67-69] However, the general multi-enzyme immobilization strategy in MOMs is not applicable to substrates with low solubilities, such as cellulose, because the enzyme@MOM composites cannot be isolated from the (unreacted) substrates and products for recycling/reuse via gravimetric separation. An alternative to enhance the separation efficiency could be via magnetic forces, as proved in our recent work wherein magnetic MOFs were prepared to encapsulate a model large-substrate enzyme; enzyme reusability was greatly enhanced via magnetic separation as compared to gravimetric separation.58

This work is a follow-up of our previous two works-- we aim at proving the concept of combining multi-enzyme immobilization in MOMs and magnetic MOFs to host cellulose carbohydrases and enhance enzyme reusability via magnetic separation, with the ultimate goal of developing magnetic biomaterials for rapid, sustainable, and low-cost degradation of plant cell walls. For proof-of-principle, we select cellulase, hemi-cellulase, and xylanase to break down the cellulose, hemi-cellulose, and short oligosaccharide bonds that dominate in a cellulose sample, respectively. These enzymes are from commercial resources so that each enzyme is not necessarily a single enzyme; details depend on the vendor as detailed in the Supporting Information (SI). In fact, cellulases and hemicellulases often contain various different enzymes (*i.e.*, endocellulase and

exocellulase both belong to cellulases) each breaks down different bonds in cellulose. To avoid such complexity, we selected the commercial resources which contain a mixture of multiple cellulases and hemicellulases in order to simplify our biocomposite preparation. Practically, most commercial enzymes possess exceptional stability (in the powder state), optimized catalytic activity, and reasonable cost. An acid/base stable MOM that can be formed in the aqueous phase while encapsulating magnetic nanoparticles (MNPs) and enzymes, Ca-BDC, is selected for enzyme immobilization, due to its relatively large and mechanically stable crystal.[53] Upon confirming each enzyme was functional in our Ca-BDC, three enzymes were encapsulated simultaneously in one Ca-BDC as confirmed structurally and functionally. The reusability was assessed via gravimetric (on Ca-BDC) and magnetic separation (on MNP-Ca-BDC), the latter of which showed significantly enhanced reusability.

This work represents the first experimental demonstration of magnetic Ca-MOMs for immobilizing multiple carbohydrases that work in a cocktail manner to degrade cellulose via magnetic forces. This work is triply meaningful for green/sustainable chemistry: 1) reusing the enzymes saves energy and resources to prepare them, 2) the synthetic conditions are "green" (ambient temperature/pressure and aqueous phase) without generating hazard wastes, and 3) the application of our multi-enzyme@MNP-Ca-BDC composites for cellulose degradation is the first step of breaking down plant cell walls and the extraction of valuable materials from sustainable resources of biomasses.

Results and Discussion

Enzyme selection and free enzyme activity assessment. The commercial cellulase (cell), hemicellulase (hemi), and xylanase (xyl) from Sigma-Aldrich were purchased for proof-of-concept in this work (biochemical/chemical supplies are presented in the Experimental Methods section

and the SI). The principles to assess the activity of each enzyme are as follows. Cellulase hydrolyzes cellulose from an undigestible matrix into glucose, which can be measured by quantifying the amount of glucose in solution. In doing so, cellulase (or corresponding enzyme@MOM composites) was mixed with the cellulose crystal and incubated at a desired temperature (ca. 37 °C) for 2 hours (we have investigated the effects of longer reaction time as well; see below discussion in the Activity of Each Enzyme@Ca-BDC Composite section). The reaction mixture was then centrifuged with the supernatant collected (since measuring cellulase activity has been made commercially available, we will not repeat the procedure in the main text; details see Experimental Methods). To measure the concentration of glucose in the supernatant, we employed the standard Glucose Assay Reagent containing adenosine triphosphate (ATP), hexokinase, nicotinamide adenine dinucleotide (NAD^+) and glucose-6-phosphate dehydrogenase (G6PDH). Herein, glucose was phosphorylated into Glucose-6-Phosphate (G6P) by ATP over time, a process catalyzed by hexokinase (Scheme 1). G6P was then oxidized by G6PDH into 6-phosphogluconate. Through this process, NAD^+ was reduced to NADH (see Scheme S1). The generation of NADH over time was then determined by measuring the absorbance at 340 nm (A340) using a standard ultra-visible (UV) spectrometer. The rise in A340 (or the slope of the A340 over time plot) was proportional to the amount of active cellulase enzyme. Representative data with 10 mM cellulase in water are shown in Figure 1 (black).

Scheme 1. Illustration of the principle to measure the concentration of glucose generated by cellulose degradation by cellulase.

Hemicellulase hydrolyzes hemicellulose. It is not very straightforward to measure hemicellulase activity using commercial kits. Instead, we found that the presence of hemicellulase improved the activity of cellulase in the cellulase activity assay as described above. Thus, the activity of hemicellulase was measured based on relative improvement of cellulase activity. Figure 1 (red) shows a typical measure of relative activity based on the comparison between a mixture of cellulase and hemicellulose (both at 10 mM) and cellulase (10 mM) alone. It is clear that the output from the mixture of hemicellulase and cellulase was higher than cellulase alone, proving the activity of hemicellulase. Same conclusion was found when cellulase and (cellulase + hemicellulase) were immobilized on Ca-BDC (see below).

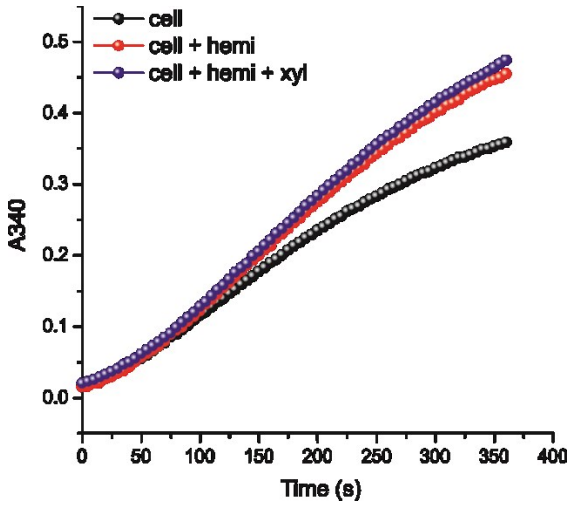

Figure 1. Free enzyme activity assays using procedures described in the main text demonstrate our operation of activity measurement. Cellulase alone (1 mM; black), a mixture of 1 mM cellulase and 1 mM hemicellulase (red), and a mixture of cellulase, hemicellulase, and xylanase (all at 1 mM; purple) all show the expected increase in A340. The presence of hemicellulase increases the activity of cellulase, confirming the activity of the former. Abbreviations: “cell” = cellulase; “hemi” = hemicellulase; “xyl” = xylanase.

Xylanase degrades xylan. The commercial xylanase assay kit contains a XylX6 reagent made up of two components: a XylX6 colorimetric substrate and β-xylosidase. The XylX6 colorimetric substrate can be hydrolyzed by the endo-xylanase, the product of which can be further hydrolyzed by the β-xylosdase, which releases the colorimetric group, 4-nitrophenol, which shows absorbance at 400 nm (A400) under alkaline pHs (Scheme 2). The amount of 4-nitrophenol release is directly related to the activity of xylanase in the solution. Using this principle, we have measured the activity of 1 mM Xylanase as detailed in Experimental Methods. Representative data using this principle are shown in the SI (Table S1). Thus, we have proved the effectiveness of each enzymatic assay for the enzymes selected in this work.

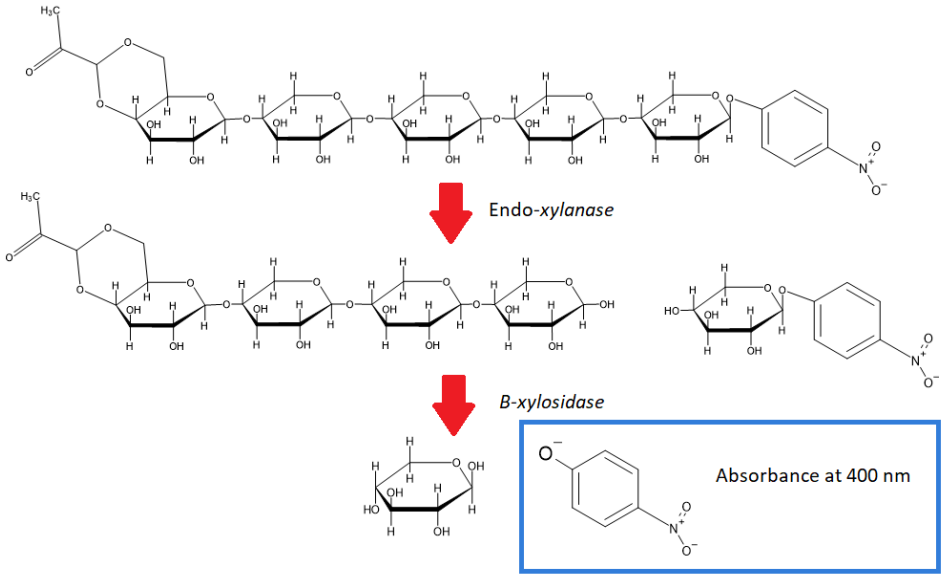

Scheme 2. Illustration of the principle to measure the activity of xylanase.

Single-Enzyme@Ca-BDC Composites. Next, we aim at proving that each enzyme is active on our Ca-BDC platform. In brief, Cell@Ca-BDC was prepared by combining 63 μL of enzyme (12

mM) and 63 μL of $CaCl_2$ (0.5 M in water) into 63 μL water. This solution was mixed via gentle pipetting. Then, 63 μL of Na_2-BDC (0.5 M in water; selection of recipe and detailed preparation see our recent works68) was added and thoroughly mixed by pipetting. All samples were incubated overnight at room temperature and washed in water for 4 times to remove any unbound reagents. Complete removal was confirmed by the UV-vis spectroscopy which can detect protein presence (A280) and BDC (A235). The same procedure was applied to prepare Hemi@Ca-BDC. To prepare xyl@Ca-BDC, the xylanase protein was mixed into water with heating due to its low solubility in water and stirring for > 20 min. The undissolved substrate was removed by filtration. A concentration of 12 mM is not achievable however, it does yield enough soluble protein (~5 mM). The same operation was then carried out to encapsulate xylanase into Ca-BDC.

The morphology and crystallinity of each enzyme@Ca-BDC composite were determined using scanning electron microscope (SEM) and powder X-ray diffraction (PXRD). SEM shows rectangular shape on the order of μm size (Figures 2 and S1), consistent with the published Ca-BDC morphology.[53] This is not a surprise because enzyme entrapment in Ca-BDC usually does not affect the size and shape of the crystal. The PXRD patterns of Ca-BDC and enzyme@Ca-DBC shown in Figure 3 (black) are consistent with those of Ca-BDC alone and Ca-BDC with other enzymes encapsulated in as published in our recent work,[57] confirming the success in preparing Ca-BDC and that encapsulation of each enzyme did not affect the crystallinity of the Ca-BDC MOM significantly. Upon encapsulation of each enzyme (and all three enzymes together), the patterns are almost superimposable with each other and that of Ca-BDC alone, suggesting that multi-enzyme entrapment did not alter the crystallinity of Ca-BDC significantly (Figure 2). The presence of each enzyme in Ca-BDC was further confirmed by confocal fluorescence imaging, wherein cellulase, hemicellulase, and xylanase were labeled with an FITC green, ATTO-520, and

ATTO-647, fluorescent probe, respectively, followed by acquiring confocal fluorescent images at 488, 520, and 647 nm as detailed in our recent work and Experimental Methods.[69] The resultant images showed the expected color for each fluoro-labeled enzyme (Figure 4 a-c) confirming the successful encapsulation of each enzyme in Ca-BDC (additional confocal images see Figure S2). The size and shape of the images are also close to those observed from SEM images. The thermal gravimetric analysis (TGA) was carried out to estimate the enzyme loading capacity. As shown in Figure S3, the weight loss from 100 to 170 °C is originated from water loss, while that from 240 to 500 °C is the loss of enzymes. The TGA data also indicated an ∼1.0% w/w of enzyme encapsulation (Figure S3) for each enzyme, which was further confirmed by protein UV absorption measurements as described before.[53, 69] The amount of loaded enzyme over the total added enzyme was roughly as ∼5%, no higher than other immobilization methods such as covalent linking or physical adsorption. However, co-crystallizing enzymes in Ca-BDC MOM prevents leaching (*versus* physical adsorption) and does not require any chemical changes to the enzyme (*versus* covalent linking).

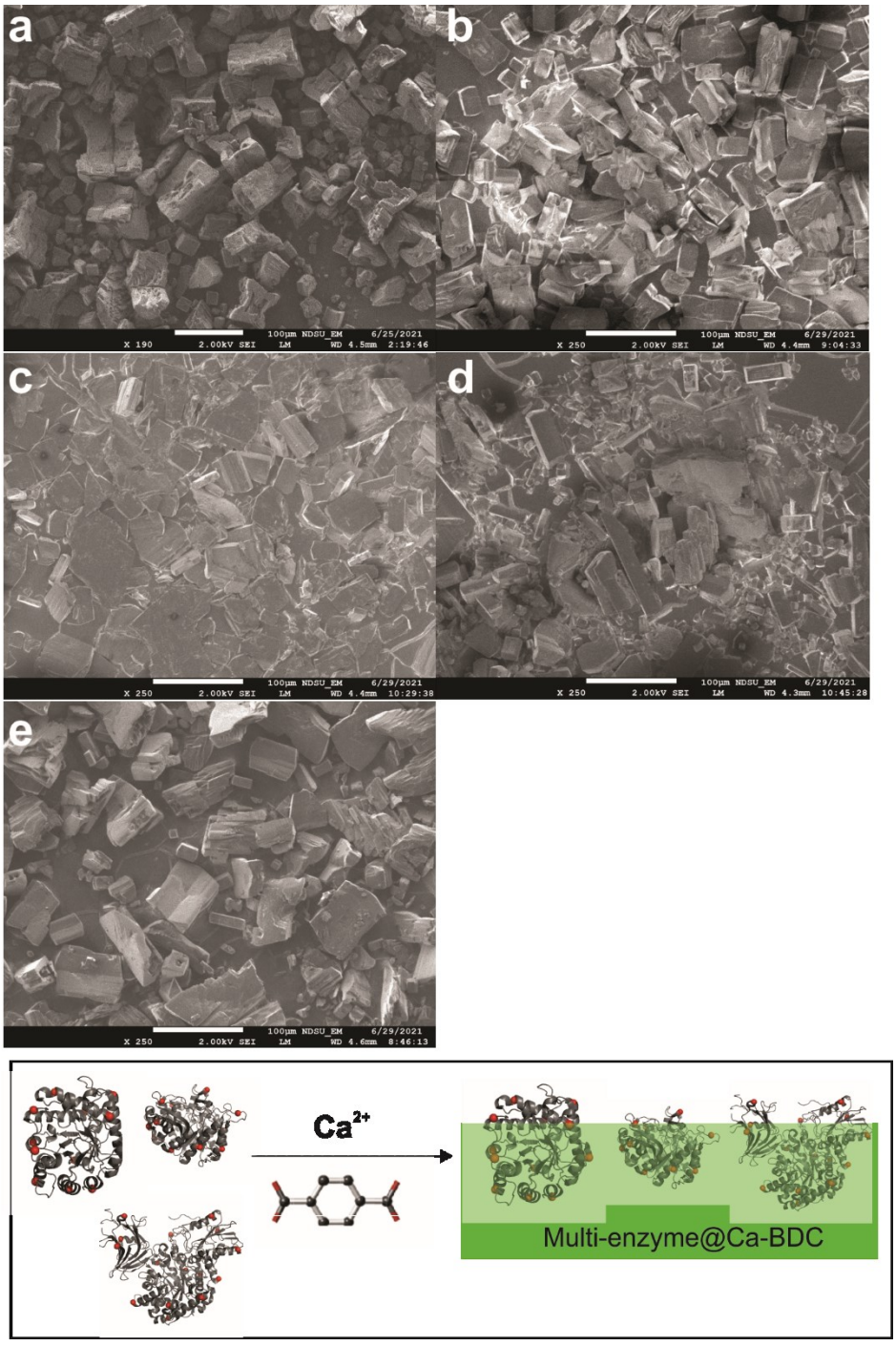

Figure 2. The SEM images of the Ca-BDC (a), Cell@Ca-BDC (b), Hemi@Ca-BDC (c), Xyl@Ca-BDC (d), and 3-in-1@Ca-BDC (e) composites prepared in this work. Overall all composites showed particles close in size and shape, which is not a surprise given the use of the same metal ion and ligand. (inset) Reaction scheme of forming the multi-enzyme@Ca-BDC

biocomposite: three enzymes that can degrade cellulose, endocellulase (PDB 4W85), exocellulase (PDB 3UT0), and cellobiase (PDB 2CBV) can be mixed with Ca^{2+} and BDC ligand to form the multi-enzyme@Ca-BDC biocomposite via aqueous-phase co-crystallization. The green shade indicates the scaffold of the Ca-BDC crystal.

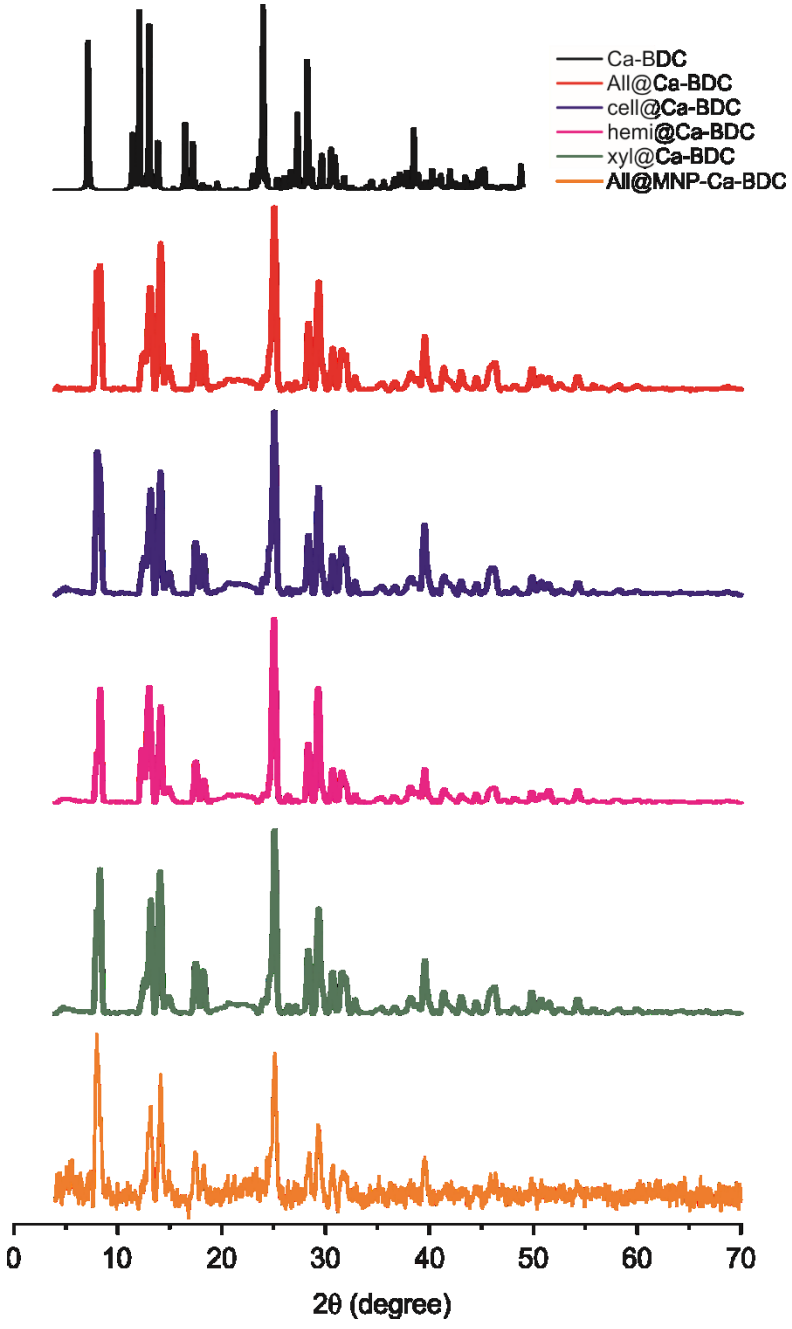

Figure 3. PXRD patterns of the Ca-BDC alone (black), 3-in-1@Ca-BDC (red), Cell@Ca-BDC (blue), Hemi@Ca-BDC (magenta), Xyl@Ca-BDC (green), and 3-in-1@MNP-Ca-BDC involved in this work. The patterns are almost superimposable over each other, except for minor broadenings when enzymes are encapsulated as compared to Ca-BDC alone.

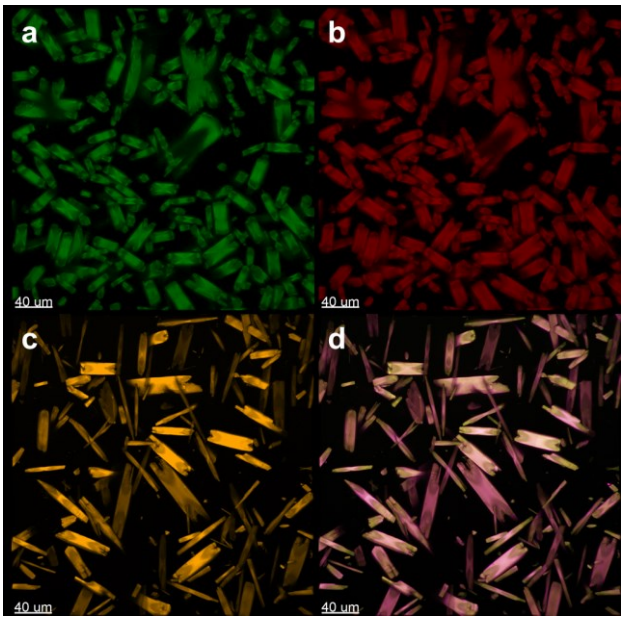

Figure 4. Confocal fluorescent images of the FITC-Cell@Ca-BDC (a), ATTO-520-Hemi@Ca-BDC (b), ATTO-647-Xyl@Ca-BDC (c), and 3-in-1@Ca-BDC (d) composites prepared in this work under the emission of 488, 520, 647, and 534 nm, respectively.

Activity of Each Enzyme@Ca-BDC Composite. The activity of each enzyme upon encapsulation into Ca-BDC was assessed using the principles described above. Upon verifying Ca^{2+}, BDC, and free Ca-BDC alone did not generate A340 (Figure S4), varied volumes of Cell@Ca-BDC composite were selected from the prepared composites and subjected for the cellulase activity test. Representative data shown in Figure S5 confirm the increase in A340, and

thus, the generation of the key product of cellulose degradation, glucose. Figure S5 also indicates that the slope of A340 increase seems to be not heavily dependent on the amount of Cell@Ca-BDC composite (roughly 10 *vs* 15 mM cellulase concentrations), suggesting that the amount of glucose that can be generated under our experimental condition was likely saturated. In other words, with excess cellulose crystals, we have reached the maximum capacity of cellulose degradation. We also noted a significant amount of cellulose crystals present after 2 hours of reaction; extending the reaction time to overnight did not change this fact. These further indicated that we have reached a "saturation" point no matter how much more time or enzyme we apply to the cellulose crystals. Or, all possible "cleavable" glucose has been cleaved off.

Representative data on varied amounts of xylanase shown in Table S1 confirmed the generation of A400 (positive control was free xylanase, while negative controls were Ca^{2+}, BDC, and free Ca-BDC alone) and thus, xylanase was active upon encapsulation in Ca-BDC. Hemi@Ca-BDC activity was assessed similarly as free enzyme and confirmed to be active as well.

We have also probed the activity dependence on pH and temperature. As shown in Figure 5, for Cell@Ca-BDC, pH 6 appeared to be the optimal pH while 35-45 ℃ is the optimal temperature range. The reason to have large difference in cellulase activity under different temperature and pH is caused by the enzyme itself. Every enzyme has an optimal working pH and temperature. Out of the optimal "zone", enzymes can display drastically different catalytic performance. For example, at pH 7 or 9, certain residues of cellulase may be deprotonated, altering the active site's charge and affinity to substrates. Although the higher the temperature, the more active the enzymes are (to bind to substrates), extremely high temperature can denature or at least partially unfold the enzyme. On solid support, because of the restriction of enzyme's free motion, the impact of pH and temperature can be higher than that in solution states. For Xyl@Ca-BDC,

the optimal pH range is 7-9 while a similar temperature range is observed (Figure S6). Overall, we chose pH 6 and 45 ℃ as the experimental condition for further experiments. Here, a unique advantage Ca-BDC offers as the enzyme immobilization platform is its wide pH stability.

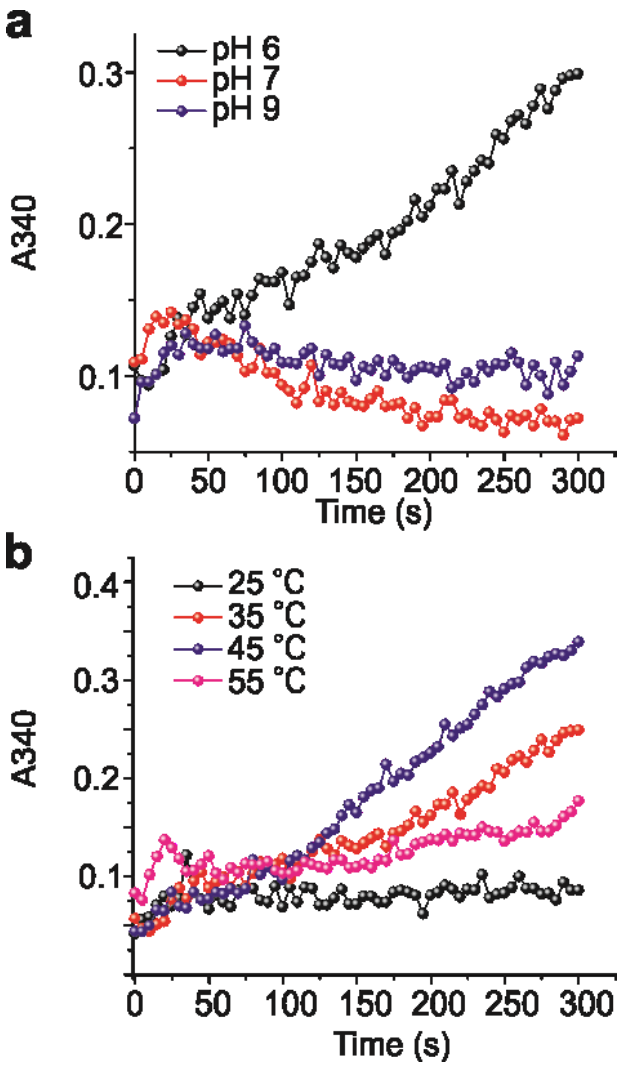

Figure 5. Cell@Ca-BDC activity under different pH (a) and temperatures (b).

Synthesis and activity of 3-in-1@Ca-BDC. To prepare the 3-in-1@Ca-BDC composites, 50 uL of each enzyme (12 mM for cell and hemi and 5 mM for xyl) was added into 63 μL of $CaCl_2$ (0.5

M) and 63 μL of BDC (0.5 M), followed by the same wash procedure to remove unbounded/unreacted species. The morphology and crystallinity of each enzyme@Ca-BDC composite were determined using SEM and PXRD. The SEM shown in Figure 2e shows a similar size and shape as compared to the single enzyme@Ca-BDC composites. The PXRD data indicate that the presence of all 3 enzymes together did not alter the crystallinity of Ca-BDC significantly (Figure 3). Confocal fluorescent image (Figure 4d) under the emission at 534 nm shows multiple colors, indicating the co-presence of three enzymes (labeled by different fluorescent probes). The thermal gravimetric analysis also confirmed the presence of 3 enzymes with roughly a loading capacity (Figure S3). We could not distinguish the loading amount of each enzyme in 3-in-1@Ca-BDC, given that the fluorescent intensity in the confocal images may not always precisely reflect the relative molar ratio or loading amount of each enzyme. Activity of each enzyme was measured individually for cellulase and in combination under varied hemicellulase amounts (Figure 6a). The data indicate that the highest activity can be achieved with the combination of cellulase, xylanase, and hemicellulase, although enhancing hemicellualse amount (by a factor of 10) did not improve the activity significantly. A similar activity dependence on pH and temperature for the 3-in-1@Ca-BDC based on cellulase and xylanase activity assays was also observed, suggesting the validity of our choice of pH 6 and 45 ℃ as the optimal reaction condition.

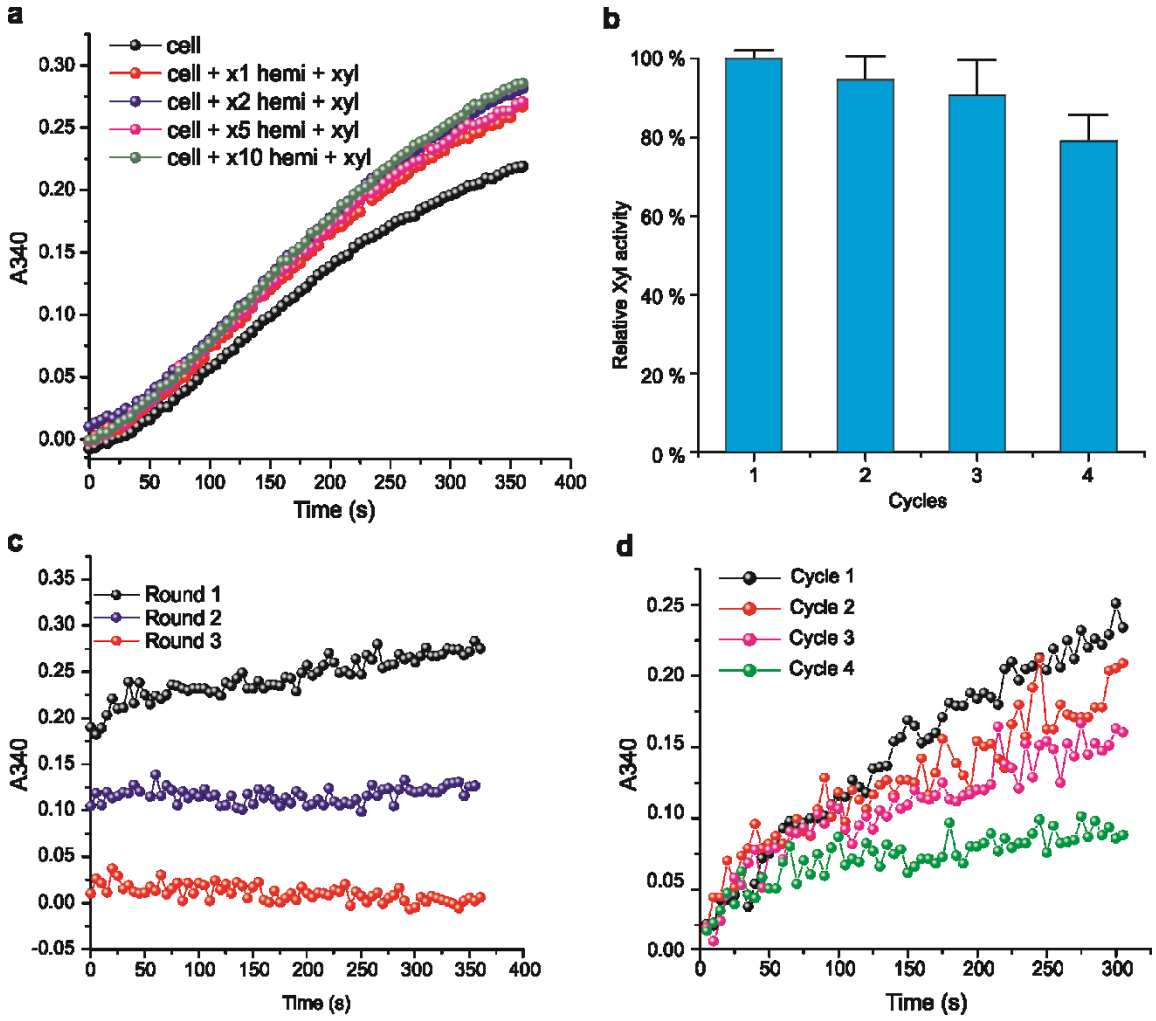

Figure 6. The activity of the 3-in-1@Ca-BDC activity probed via the cellulase activity assay (a) and reusability determined via xylanase (b) and cellulase activity assays (c), respectively. Error bars in (b) were calculated based on three repeated measurements of the xylanase activity when the 3-in-1@Ca-BDC composite was applied to the xylanase activity kit. The y-axis in (c) has been shifted by ~0.10 among different rounds of reuse. (d) The reusability of the 3-in-1@MNP-Ca-BDC tested using the cellulase activity assay. In comparison to (c), the presence of MNPs significantly enhanced the reusability of the involved enzymes.

Reusability of the 3-in-1@Ca-BDC composite was first assessed using the xylanase activity assay due to the good solubility of substrates and products, by measuring A400 using the xylanase activity kit, retrieving the 3-in-1@Ca-BDC composite via centrifugation, washing, and repeating the same operations. Results of this experiment showed that activity was presented for at least 4 cycles (Figure 6b). The activity was reduced slightly with each cycle; however, this may be attributed to the possible loss of product from continued washing.

We have also attempted to assess the reusability of our 3-in-1@Ca-BDC composites using the cellulose activity assay. However, we found it quite difficult to retrieve our composites from the insoluble, unreacted cellulose crystals, and/or insoluble by-products, as these are all pellets after one round of reaction. We therefore initiated a second round of reaction by adding in more cellulose crystals (a few mg) and found near undetectable generation of glucose. This could be caused by the fact that the active sites of cellulase on 3-in-1@Ca-BDC were blocked by the insoluble products of the first round of reaction. Representative data are shown in Figure 6c. These data suggested abysmal reusability of our 3-in-1@Ca-BDC composites.

One attempt to solve this problem was to try to the cellulose crystal substrates as much as possible. However, we have extended reaction time significantly and still could not make all products soluble in water. We have also attempted to solubilize cellulose by heating and adjusting pHs. However, this attempt was not successful either. Lastly, we have attempted to significantly reduce the initial amount of substrate, with the hope of completely degrading them. However, as the amount of cellulose was decreased, the generated glucose was also dropped rapidly below the detection limit. Thus, all our attempts to assess the reusability of our 3-in-1@Ca-BDC composites using the cellulase activity kit failed. Although we can still claim that our 3-in-1@Ca-BDC composites are reusable based on xylanase activity tests, not being able to recovery/retrieve our

composites from the insoluble products and unreacted substrates significantly dampened the application possibility of our 3-in-1@Ca-BDC composites. An alternative strategy of isolation/separation is needed.

Magnetic separation. In principle, magnetic forces should be able to separate magnetic particles from diamagnetic ones under a strong external magnet, as proved in our recent work.[58] We therefore adapted this concept in cellulose degradation. Following our recent procedures, we have included MNPs during the co-crystallization of our enzymes and Ca-BDC (details see the SI). The resultant 3-in-1@MNP-Ca-BDC composites were subjected for SEM (Figure 7) and PXRD (Figure 3 orange), which all indicate that the presence of MNPs did not significantly alter the structure of 3-in-1@MOM composites. Each enzyme was confirmed to be active in our MNP-CaBDC too using procedures detailed in Activity of Each Enzyme@Ca-BDC Composite.

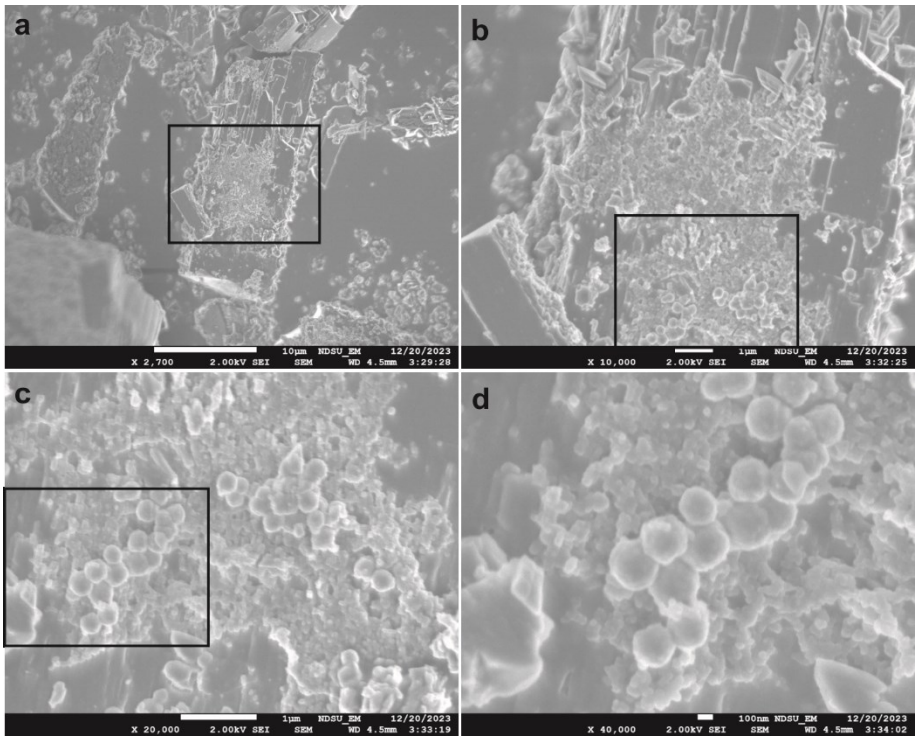

Figure 7. SEM images of our MNP-Ca-BDC with 2,700 x magnification (a), 10,000 x magnification (b), 20,000 x magnification (c), and 40,000 x magnification (d).

The resultant 3-in-1@MNP-Ca-BDC composite was found to be separable from insoluble and non-magnetic crystals under stirring by a strong external magnet (details similar to those presented in our recent work).[58] Then, via the same cellulase activity assay, we observed noticeable reusability for at least three rounds as compared to the gravimetric separation (Figure 6d *vs* 6c). In fact, our 3-in-1@MNP-Ca-BDC composite is reusable for >80 % for at least 3 cycles, which is a significant improvement, bearing in mind that our recycling efficiency can be improved via better mixing and stronger external magnets which help minimize the sample loss during the separation. Furthermore, the synthetic recipe (enzyme compositions), conditions, and MNP preparation can also be further optimized, which together will generate optimal magnetic MOMs for better enzyme reuse in cellulose degradation. Other approaches to further increase the reusability and cellulose degradation efficiency include utilizing a MOM with a much higher thermal stability (so that higher reaction temperature may be applied to help cellulose suspension and enhance enzyme reactivity), better pre-treatment of cellulose substrates (to enhance contact with our multi-enzyme@MOM composites), and including more active variants of enzymes or enzymes from different organisms. These directions are in fact our on-going research. This work is solely to show the exciting power of magnetic separation in cellulose degradation!

Cellulase and hemicellulase enzymes have molecular weights of ~60-80 kDa with a size of ~ 5 x 5 x 20 nm depending on species and organisms and a pI (isoelectric point) of ~8. Xylanase has a molecular weight of ~30 kDa with a pI of ~8-9.5. Therefore, none of the three enzymes can enter the pores of Ca-BDC, which are on the order of sub-nm. We have also attempted to directly

load each enzyme into pre-formed Ca-BDC and magnetic Ca-BDC yet after wash, there was no activity observed, suggesting these enzymes cannot be directly loaded into Ca-BDC pores. Co-crystallization is needed.

Conclusion

We demonstrated the feasibility of using co-crystallization to immobilize multiple enzymes essential for the degradation of cellulose crystals. In aqueous phase 3 enzymes were immobilized individually as well as simultaneously on to a MOM formed by Ca^{2+} and a carboxylate ligand, BDC. The presence of enzyme(s) did not alter the morphology and crystallinity of the Ca-BDC. The presence of enzyme was confirmed structurally via confocal fluorescence imaging and functionally via standard catalytic activity assays, respectively. The loading capacity was evaluated via TGA and found close to the expected enzyme loading capacity. Upon optimizing the temperature and pH of each single-enzyme@Ca-BDC, we chose the optimal condition to assess the effectiveness of the composite that contained all three enzymes. The co-presence of 3 enzymes enhanced the efficiency of cellulose degradation, and the reusability of the 3-in-1@Ca-BDC composite was found reasonable via the xylanase activity assay. However, the difficulty in separating the insoluble by-products and unreacted cellulose crystal substrates made it impossible to assess the reusability of 3-in-1@Ca-BDC composites via the cellulase activity assay. Furthermore, not being able to retrieve and recycle the 3-in-1@Ca-BDC composites after one round of cellulose degradation place a high barrier of the application of our composites. Thus, we explored the possibility using magnetic forces to separate the 3-in-1@Ca-BDC composites from insoluble portions after each round of reaction. We found close to 80% reusability from the 3-in-1@MNP-CaBDC composites via magnetic separation, which is a significant improvement as compared to the abysmal reusability via gravimetric separation. This work demonstrates for the

first time that MOFs can used to immobilize carbohydrase enzymes and degrade large, rigid biological substrate, cellulose crystals. The application of our multi-enzyme@MNP-MOF composites on biocompatible, selective, and efficient degradation of plant products offers a "green" approach to extract valuable materials from sustainable resources of plants which do not rely on non-regeneratable resources.

Experimental Methods

All supplies of chemicals and biochemicals were purchased from commercial sources in high purity without further sample processing and purification, unless described in the SI. All characterization of the involved (multi-)enzyme@Ca-BDC MOM co-crystal powders, such as PXRD, SEM, TGA, and confocal fluorescence imaging, follows the procedures published in the main text or the SI using equipment detailed in our recent work.[24] The biocatalytic activity studies of the enzymes and (multi-)enzyme@MOM composites were carried out using standard activity assays as detailed below and in the SI.

1. Cellulase activity: Cellulase (1 mM, 63 uL) was mixed with cellulose crystal (5% w/v, 4 mL) and incubated at 37 °C for 2 hours. The reaction mixtures were then centrifuged (for 1 min at 4000 G), and the supernatant was collected. To measure the concentration of glucose in the supernatant, we employed Glucose Assay Reagent (containing ATP, hexokinase, NAD^+ and G6PDH; principle see Results and Discussion). The concentration of NADH was then determined by measuring the A340. Absorbance was recorded immediately after mixing supernatant and glucose assay reagent and every 5 seconds for 5 minutes.

2. Xylanase activity: The xylanase activity assay was conducted by preparing a solution of xylanase enzyme in an extraction buffer (100 mM sodium phosphate, 0.5 mg/mL BSA, 0.02% w/v sodium azide, pH 6.0). Xylanase is challenging to dissolve. We therefore heated the solution to

~80°C and stirred for >20 minutes. 0.05 mL aliquots of XylX6 reagent solution were then dispensed to 13 mL glass tubes and preincubated at 40°C. The xylanase solution was preincubated at 40°C as well. 50 uL of xylanase was then added to the XylX6, mixed thoroughly, and incubated at 40°C for exactly 10 minutes. After 10 minutes, 1.5 mL of stopping reagent (2% w/v, Tris buffer, pH 10.0) was added and the absorbance is read at 400 nm (principle see Results and Discussion).

3. Scanning electron microscope (SEM): Typically, dried Ca-BDC, single- enzyme@Ca-BDC composites and 3-in-1@Ca-BDC composites were attached on aluminum mounts using carbon adhesive tabs/tape and then coated with a conductive layer of carbon in a high-vacuum evaporative coater (Cressington 208c, Ted Pella Inc., Redding, California, USA). The morphology of the composites was acquired using a JEOL JSM-7600F scanning electron microscope (JEOL USA Inc., Peabody, Massachusetts) operating at 2 kV.

4. **Powder X-ray diffraction (PXRD):** The dried sample was loaded into borosilicate capillary tube (0.6 mm i.d./ 0.8 mm o.d.; Wilmad Labglass, Inc.). PXRD data were collected on a Bruker AXSD8 Advance A25 Powder X-ray diffractometer (40 kV, 40 mA) using Cu Ka (l = 1.5406 Å) radiation.

5. Fluorescent labeling of protein and Confocal: Cellulase (10 mM, 1.5 mL) in carbonate-bicarbonate buffer (50 mM, pH = 9.2)) and FITC (5 µL, 10mg/mL in DMSO), hemicellulase (10 mM, 1.5 mL) in carbonate-bicarbonate buffer (50 mM, pH = 9.2)) and Atto520 (5 µL, 2mg/mL in DMSO), as well as xylanase (10 mM, 1.5 mL) in carbonate-bicarbonate buffer (50 mM, pH = 9.2)) and Atto647 (5 µL, 2mg/mL in DMSO) were incubated at ambient temperature overnight under shanking. Excess dyes were removed using the Amicon spin concentrator (Millipore, 3,000 MWCO / 10,000 MWCO / 30,000 MWCO, 50 mL). The obtained dye-enzymes were covered with foil and stored at 4 ºC for further use. For confocal experiments, dye-enzymes were entrapped into

Ca-BDC composite as described above (see above), followed by washing with deionized water. Upon dispersing the sample into methanol, confocal microscopy images were acquired on a Zeiss Axio observer Z1 LSM 700 confocal laser-scanning microscope (Peabody, MA). The images were processed using Imarisx64 9.0.2 software by Bitplane AG (Concord, MA).

6. TGA: TGA was measured using a Thermogravimetric Analyzer (TGA), TA Instruments Q500. Typically, ~ 20 mg sample was measured between 25 °C to 900 °C at a heating rate of 10 °C/min under a 40 mL/min nitrogen flow. Prior to any measurement, the samples were dried in an oven at 110 °C to remove water or other solvents.

7. MNP and MNP-Ca-BDC: Fe_3O_4 was synthesized following the published solve-thermal method with slight modification.[70] Briefly, 2.235 g of $FeCl_3$•$6H_2O$ was completely dissolved in 50 mL of ethylene glycol under gentle stirring, followed by addition of 0.578 g of sodium citrate and 3.435 g of sodium acetate. The transparent mixture was obtained after vigorously stirring for 30 min, and further transferred to a Teflon-lined stainless-steel autoclave and incubated at 200 ºC for 8 h. The produced black magnetic nanoparticles were washed with dd-water, and collected with magnet and dried at 60 ºC for 6 h.

5 µL of 27.6 mg/mL Fe_3O_4 MNP was dispersed into 300 µL of dd-water under ultrasonication for 5 min, following by addition of 5 µL (1 mM) of cellulase, hemicellulase, and xylanase, and 300 µL of 0.5 M of $CaCl_2$ and BDC. The mixture was immediately mixed well by vigorous vortex and then incubated at ambient temperature for 12 h. The obtained enzyme@MNP-CaBDC was washed with dd-water for 3 times and resuspend in 100 µL of H_2O for characterization.

Acknowledgements

This work is supported by the National Science Foundation (NSF MCB 1942596 and NSF DMR 2306137 to Z. Y. as well as NSF CHE 2050802 to G.N. and J. W.).

Supporting Information

Resources of chemical supplies, details of (multi-)enzyme@MOM composite synthesis, basic characterization of the prepared composites, TGA data, raw data of enzyme activity assay, and controls, as well as supporting tables of experimental data.

References

1. McKendry, P., Energy production from biomass (part 1): overview of biomass. *Bioresour. Technol.* **2002,** *83* (1), 37-46.
2. McKendry, P., Energy production from biomass (part 2): conversion technologies. *Bioresour. Technol.* **2002,** *83* (1), 47-54.
3. Luzier, W. D., Materials derived from biomass/biodegradable materials. *Proc. Natl. Acad. Sci.* **1992,** *89* (3), 839.
4. Zhang, L.; Liu, Z.; Cui, G.; Chen, L., Biomass-derived materials for electrochemical energy storages. *Prog. Polym. Sci.* **2015,** *43*, 136-164.
5. Varma, R. S., Biomass-Derived Renewable Carbonaceous Materials for Sustainable Chemical and Environmental Applications. *ACS Sustain. Chem. Eng.* **2019,** *7* (7), 6458-6470.
6. Baratieri, M.; Baggio, P.; Fiori, L.; Grigiante, M., Biomass as an energy source: Thermodynamic constraints on the performance of the conversion process. *Bioresour. Technol.* **2008,** *99* (15), 7063-7073.
7. Guerriero, G.; Hausman, J.-F.; Strauss, J.; Ertan, H.; Siddiqui, K. S., Lignocellulosic biomass: Biosynthesis, degradation, and industrial utilization. *Eng. Life Sci.* **2016,** *16* (1), 1-16.
8. Banerjee, G.; Scott-Craig, J. S.; Walton, J. D., Improving Enzymes for Biomass Conversion: A Basic Research Perspective. *BioEnergy Res.* **2010,** *3* (1), 82-92.
9. Magdalena, J. A.; Ballesteros, M.; González-Fernandez, C. Efficient Anaerobic Digestion of Microalgae Biomass: Proteins as a Key Macromolecule *Molecules* [Online], 2018.
10. Chen, C.-C.; Dai, L.; Ma, L.; Guo, R.-T., Enzymatic degradation of plant biomass and synthetic polymers. *Nat. Rev. Chem.* **2020,** *4* (3), 114-126.
11. Stöcker, M., Biofuels and Biomass-To-Liquid Fuels in the Biorefinery: Catalytic Conversion of Lignocellulosic Biomass using Porous Materials. *Angew. Chem. Inter. Ed.* **2008,** *47* (48), 9200-9211.
12. Adsul, M.; Tuli, D. K.; Annamalai, P. K.; Depan, D.; Shankar, S., Polymers from Biomass: Characterization, Modification, Degradation, and Applications. *Inter. J. Polym. Sci.* **2016,** *2016*, 1857297.

13. Kruse, A.; Gawlik, A., Biomass Conversion in Water at 330-410 °C and 30-50 MPa. Identification of Key Compounds for Indicating Different Chemical Reaction Pathways. *Indust. Eng. Chem. Res.* **2003,** *42* (2), 267-279.
14. Eom, I.-Y.; Kim, J.-Y.; Kim, T.-S.; Lee, S.-M.; Choi, D.; Choi, I.-G.; Choi, J.-W., Effect of essential inorganic metals on primary thermal degradation of lignocellulosic biomass. *Bioresour. Technol.* **2012,** *104*, 687-694.
15. Ranzi, E.; Corbetta, M.; Manenti, F.; Pierucci, S., Kinetic modeling of the thermal degradation and combustion of biomass. *Chem. Eng. Sci.* **2014,** *110*, 2-12.
16. Ranzi, E.; Cuoci, A.; Faravelli, T.; Frassoldati, A.; Migliavacca, G.; Pierucci, S.; Sommariva, S., Chemical Kinetics of Biomass Pyrolysis. *Energy & Fuels* **2008,** *22* (6), 4292-4300.
17. Bornscheuer, U.; Buchholz, K.; Seibel, J., Enzymatic Degradation of (Ligno)cellulose. *Angew. Chem. Inter. Ed.* **2014,** *53* (41), 10876-10893.
18. Schrittwieser, J. H.; Velikogne, S.; Hall, M.; Kroutil, W., Artificial Biocatalytic Linear Cascades for Preparation of Organic Molecules. *Chem. Rev.* **2018,** *118* (1), 270-348.
19. Quinlan, R. J.; Sweeney, M. D.; Lo Leggio, L.; Otten, H.; Poulsen, J.-C. N.; Johansen, K. S.; Krogh, K. B. R. M.; Jorgensen, C. I.; Tovborg, M.; Anthonsen, A.; Tryfona, T.; Walter, C. P.; Dupree, P.; Xu, F.; Davies, G. J.; Walton, P. H., Insights into the oxidative degradation of cellulose by a copper metalloenzyme that exploits biomass components. *Proc. Natl. Acad. Sci.* **2011,** *108* (37), 15079.
20. Banerjee, A.; Chatterjee, K.; Madras, G., Enzymatic degradation of polymers: a brief review. *Mater. Sci. Technol.* **2013,** *30* (5), 567-573.
21. Roohi; Kulsoom, B.; Mohammed, K.; Mohammed, R. Z.; Qamar, Z.; Mohammed, F. K.; Ghulam Md, A.; Anamika, G.; Gjumrakch, A., Microbial Enzymatic Degradation of Biodegradable Plastics. *Curr. Pharm. Biotechnol.* **2017,** *18* (5), 429-440.
22. Bisaria, V. S.; Ghose, T. K., Biodegradation of cellulosic materials: Substrates, microorganisms, enzymes and products. *Enzyme Microb. Technol.* **1981,** *3* (2), 90-104.
23. Dutta, S.; Wu, K. C. W., Enzymatic breakdown of biomass: enzyme active sites, immobilization, and biofuel production. *Green Chem.* **2014,** *16* (11), 4615-4626.
24. Horn, S. J.; Vaaje-Kolstad, G.; Westereng, B. r.; Eijsink, V., Novel enzymes for the degradation of cellulose. *Biotechnol. Biofuels* **2012,** *5* (1), 45.
25. Himmel, M. E.; Ding, S.-Y.; Johnson, D. K.; Adney, W. S.; Nimlos, M. R.; Brady, J. W.; Foust, T. D., Biomass Recalcitrance: Engineering Plants and Enzymes for Biofuels Production. *Science* **2007,** *315* (5813), 804.
26. Yang, B.; Dai, Z.; Ding, S.-Y.; Wyman, C. E., Enzymatic hydrolysis of cellulosic biomass. *Biofuels* **2014,** *2* (4), 421-449.
27. Merino, S. T.; Cherry, J., Progress and Challenges in Enzyme Development for Biomass Utilization. In *Biofuels*, Springer Berlin Heidelberg: Berlin, Heidelberg, 2007; pp 95-120.
28. Wang, Y.; Ren, H.; Zhao, H., Expanding the boundary of biocatalysis: design and optimization of in vitro tandem catalytic reactions for biochemical production. *Crit. Rev. Biochem. Mol. Biol.* **2018,** *53* (2), 115-129.
28. Muschiol, J.; Peters, C.; Oberleitner, N.; Mihovilovic, M. D.; Bornscheuer, U. T.; Rudroff, F., Cascade catalysis: strategies and challenges en route to preparative synthetic biology. *Chem. Commun.* **2015,** *51* (27), 5798-5811.
30. Göβl, D. e.; Singer, H.; Chiu, H.-Y.; Schmidt, A.; Lichtnecker, M.; Engelke, H.; Bein, T., Highly active enzymes immobilized in large pore colloidal mesoporous silica nanoparticles. *New J. Chem.* **2019,** *43* (4), 1671-1680.

31. Nabavi Zadeh, P. S.; Åkerman, B., Immobilization of Enzymes in Mesoporous Silica Particles: Protein Concentration and Rotational Mobility in the Pores. *J. Phys. Chem. B* **2017,** *121* (12), 2575-2583.
32. Bolivar, J. M.; Eisl, I.; Nidetzky, B., Advanced characterization of immobilized enzymes as heterogeneous biocatalysts. *Catal. Today* **2016,** *259*, 66-80.
33. Carlsson, N.; Gustafsson, H.; Thörn, C.; Olsson, L.; Holmberg, K.; Åkerman, B., Enzymes immobilized in mesoporous silica: A physical-chemical perspective. *Adv. Colloid Interface Sci.* **2014,** *205*, 339-360.
34. Zhou, Z.; Hartmann, M., Progress in enzyme immobilization in ordered mesoporous materials and related applications. *Chem. Soc. Rev.* **2013,** *42* (9), 3894-3912.
35. Magner, E., Immobilisation of enzymes on mesoporous silicate materials. *Chem. Soc. Rev.* **2013,** *42* (15), 6213-6222.
36. Popat, A.; Hartono, S. B.; Stahr, F.; Liu, J.; Qiao, S. Z.; Qing Lu, G., Mesoporous silica nanoparticles for bioadsorption, enzyme immobilisation, and delivery carriers. *Nanoscale* **2011,** *3* (7), 2801-2818.
37. Lee, C.-H.; Lin, T.-S.; Mou, C.-Y., Mesoporous materials for encapsulating enzymes. *Nano Today* **2009,** *4* (2), 165-179.
38. Sheldon, R. A.; van Pelt, S., Enzyme immobilisation in biocatalysis: why, what and how. *Chem. Soc. Rev.* **2013,** *42* (15), 6223-6235.
39. Sheldon, R. A., Enzyme Immobilization: The Quest for Optimum Performance. *Adv. Syn. Catal.* **2007,** *349* (8-9), 1289-1307.
40. Datta, S.; Christena, L. R.; Rajaram, Y. R. S., Enzyme immobilization: an overview on techniques and support materials. *3 Biotech* **2013,** *3* (1), 1-9.
41. Li, P.; Chen, Q.; Wang, T. C.; Vermeulen, N. A.; Mehdi, B. L.; Dohnalkova, A.; Browning, N. D.; Shen, D.; Anderson, R.; Gómez-Gualdrón, D. A.; Cetin, F. M.; Jagiello, J.; Asiri, A. M.; Stoddart, J. F.; Farha, O. K., Hierarchically Engineered Mesoporous Metal-Organic Frameworks toward Cell-free Immobilized Enzyme Systems. *Chem* **2018,** *4* (5), 1022-1034.
42. Majewski, M. B.; Howarth, A. J.; Li, P.; Wasielewski, M. R.; Hupp, J. T.; Farha, O. K., Enzyme encapsulation in metal-organic frameworks for applications in catalysis. *CrystEngComm* **2017,** *19* (29), 4082-4091.
43. Drout, R. J.; Robison, L.; Farha, O. K., Catalytic applications of enzymes encapsulated in metal-organic frameworks. *Coord. Chem. Rev.* **2019,** *381*, 151-160.
44. Howarth, A. J.; Liu, Y.; Li, P.; Li, Z.; Wang, T. C.; Hupp, J. T.; Farha, O. K., Chemical, thermal and mechanical stabilities of metal-organic frameworks. *Nat. Rev. Mater.* **2016,** *1*, 15018.
45. Fang, Y.; Powell, J. A.; Li, E.; Wang, Q.; Perry, Z.; Kirchon, A.; Yang, X.; Xiao, Z.; Zhu, C.; Zhang, L.; Huang, F.; Zhou, H.-C., Catalytic reactions within the cavity of coordination cages. *Chem. Soc. Rev.* **2019,** *48* (17), 4707-4730.
46. Lian, X.; Fang, Y.; Joseph, E.; Wang, Q.; Li, J.; Banerjee, S.; Lollar, C.; Wang, X.; Zhou, H.-C., Enzyme-MOF (metal-organic framework) composites. *Chem. Soc. Rev.* **2017,** *46* (11), 3386-3401.
47. Liang, K.; Ricco, R.; Doherty, C. M.; Styles, M. J.; Bell, S.; Kirby, N.; Mudie, S.; Haylock, D.; Hill, A. J.; Doonan, C. J.; Falcaro, P., Biomimetic mineralization of metal-organic frameworks as protective coatings for biomacromolecules. *Nat. Commun.* **2015,** *6*, 7240.
48. Doonan, C.; Riccò, R.; Liang, K.; Bradshaw, D.; Falcaro, P., Metal-Organic Frameworks at the Biointerface: Synthetic Strategies and Applications. *Acc. Chem. Res.* **2017,** *50* (6), 1423-1432.

49. Wang, X.; Lan, P. C.; Ma, S., Metal-Organic Frameworks for Enzyme Immobilization: Beyond Host Matrix Materials. *ACS Centr. Sci.* **2020**, *6*, 1497-1506.
50. Sun, Q.; Pan, Y.; Wang, X.; Li, H.; Farmakes, J.; Aguila, B.; Yang, Z.; Ma, S., Mapping out the Degree of Freedom of Hosted Enzymes in Confined Spatial Environments. *Chem* **2019,** *5* (12), 3184-3195.
51. Chen, Y.; Lykourinou, V.; Vetromile, C.; Hoang, T.; Ming, L. J.; Larsen, R. W.; Ma, S., How can proteins enter the interior of a MOF? investigation of cytochrome c translocation into a MOF consisting of mesoporous cages with microporous windows. *J. Am. Chem. Soc.* **2012,** *134* (32), 13188-13191.
52. Song, Y.; Sun, Q.; Aguila, B.; Ma, S., Opportunities of Covalent Organic Frameworks for Advanced Applications. *Adv. Sci.* **2019,** *6* (2), article no. 1801410.
53. Pan, Y.; Li, Q.; Li, H.; Farmakes, J.; Ugrinov, A.; Zhu, X.; Lai, Z.; Chen, B.; Yang, Z., A General Ca-MOM Platform with Enhanced Acid/Base Stability for Enzyme Biocatalysis. *Chem Catal.* **2021,** *1*, 146-161.
54. Pan, Y.; Li, H.; Farmakes, J.; Xiao, F.; Chen, B.; Ma, S.; Yang, Z., How Do Enzymes Orient on Metal-Organic Framework (MOF) Surfaces? *J. Am. Chem. Soc.* **2018,** *140*, 16032-16036.
55. Pan, Y.; Li, H.; Lenertz, M.; Han, Y.; Ugrinov, A.; Kilin, D.; Chen, B.; Yang, Z., One-pot Synthesis of Enzyme@Metal-Organic Materials (MOM) Biocomposites for Enzyme Biocatalysis. *Green Chem.* **2021,** *33*, 4466-4476.
56. Farmakes, J.; Schuster, I.; Overby, A.; Alhalhooly, L.; Lenertz, M.; Li, Q.; Ugrinov, A.; Choi, Y.; Pan, Y.; Yang, Z., Enzyme immobilization on graphene oxide (GO) surface via one-pot synthesis of GO/metal-organic framework composites for large-substrate biocatalysis. *ACS Appl. Mater. Interfaces* **2020,** *12* (20), 23119-23126.
57. Neupane, S.; Patnode, K.; Li, H.; Baryeh, K.; Liu, G.; Hu, J.; Chen, B.; Pan, Y.; Yang, Z., Enhancing Enzyme Immobilization on Carbon Nanotubes via Metal-Organic Frameworks for Large-Substrate Biocatalysis. *ACS Appl. Mater. Interfaces* **2019,** *11* (12), 12133-12141.
58. Li, Q.; Pan, Y.; Li, H.; Alhalhooly, L.; Li, Y.; Chen, B.; Choi, Y.; Yang, Z., Size-tunable Metal-Organic Framework Coated Magnetic Nanoparticles for Enzyme Encapsulation and Large-Substrate Biocatalysis. *ACS Appl. Mater. Interfaces* **2020,** *12*, 41794-41801.
59. Lyu, F.; Zhang, Y.; Zare, R. N.; Ge, J.; Liu, Z., One-Pot Synthesis of Protein-Embedded-Supporting Information. *Nano Lett.* **2014,** *14* (10), 5761-5765.
60. Wei, T.-H.; Wu, S.-H.; Huang, Y.-D.; Lo, W.-S.; Williams, B. P.; Chen, S.-Y.; Yang, H.-C.; Hsu, Y.-S.; Lin, Z.-Y.; Chen, X.-H.; Kuo, P.-E.; Chou, L.-Y.; Tsung, C.-K.; Shieh, F.-K., Rapid mechanochemical encapsulation of biocatalysts into robust metal-organic frameworks. *Nat. Commun.* **2019,** *10* (1), 5002.
61. Garzón-Tovar, L.; Carné-Sánchez, A.; Carbonell, C.; Imaz, I.; Maspoch, D., Optimised room temperature, water-based synthesis of CPO-27-M metal-organic frameworks with high space-time yields. *J. Mater. Chem. A* **2015,** *3* (41), 20819-20826.
62. Espín, J.; Garzón-Tovar, L.; Carné-Sánchez, A.; Imaz, I.; Maspoch, D., Photothermal Activation of Metal-Organic Frameworks Using a UV-Vis Light Source. *ACS Appl. Mater. Interfaces* **2018,** *10* (11), 9555-9562.
63. Vornholt, S. M.; Henkelis, S. E.; Morris, R. E., Low temperature synthesis study of metal-organic framework CPO-27: investigating metal, solvent and base effects down to -78 °C. *Dalton Trans.* **2017,** *46* (25), 8298-8303.
64. Reinsch, H., "Green" Synthesis of Metal-Organic Frameworks. *Euro. J. Inorg. Chem.* **2016,** *2016* (27), 4290-4299.

65. Cattaneo, D.; Warrender, S. J.; Duncan, M. J.; Castledine, R.; Parkinson, N.; Haley, I.; Morris, R. E., Water based scale-up of CPO-27 synthesis for nitric oxide delivery. *Dalton Trans.* **2016,** *45* (2), 618-629.
66. Sánchez-Sánchez, M.; Getachew, N.; DÃíaz, K.; Díaz-García, M.; Chebude, Y.; Díaz, I., Synthesis of metal-organic frameworks in water at room temperature: salts as linker sources. *Green Chem.* **2015,** *17* (3), 1500-1509.
67. Li, Q.; Armstrong, Z.; Ugrinov, A.; Chen, B.; Liu, B.; Li, H.; Pan, Y.; Yang, Z., Metal-Organic Materials Enhance Proteolytic Selectivity, Efficiency, and Reusability of Trypsin: A Time-Resolved Study on Proteolysis. *ACS Appl. Mater. Interfaces* **2022,** *15* (7), 8927-8936.
68. Jordahl, D.; Armstrong, Z.; Li, Q.; Gao, R.; Liu, W.; Johnson, K.; Brown, W.; Scheiwiller, A.; Feng, L.; Ugrinov, A.; Mao, H.; Chen, B.; Quadir, M.; Pan, Y.; Li, H.; Yang, Z., Expanding the library of Metal-Organic Frameworks (MOFs) for enzyme biomineralization. *ACS Appl. Mater. Interfaces* **2022,** *14* (46), 51619-51629.
69. Li, Q.; Pan, Y.; Li, H.; Lenertz, M.; Reed, K.; Jordahl, D.; Bjerke, T.; Ugrinov, A.; Chen, B.; Yang, Z., Cascade/parallel biocatalysis via multi-enzyme encapsulation on Metal-Organic Materials for rapid and sustainable biomass degradation. *ACS Appl. Mater. Interfaces* **2021,** *13*, 43085–43093.
70. Zheng, J.; Cheng, C.; Fang, W.-J.; Chen, C.; Yan, R.-W.; Huai, H.-X.; Wang, C.-C., Surfactant-free synthesis of a Fe3O4@ZIF-8 core-shell heterostructure for adsorption of methylene blue. *CrystEngComm* **2014,** *16* (19), 3960-3964.

TOC Figure

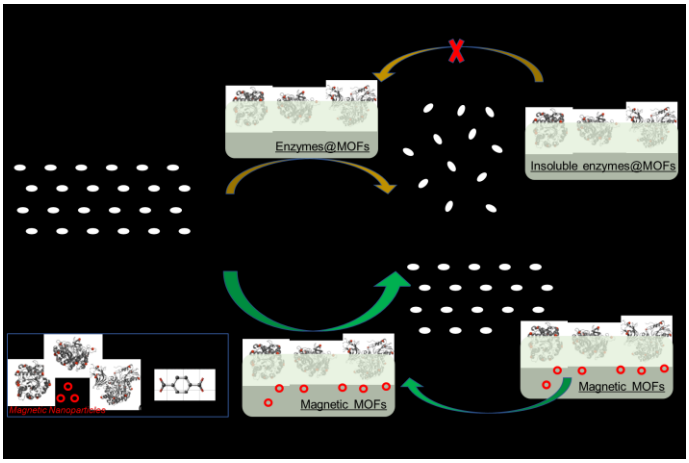
Enzymes@MOFs
Insoluble enzymes@MOFs
Magnetic MOFs
Magnetic MOFs